JOURNAL OF Applied Polymer SCIENCE

Effects of the Processing Temperature on the Nanostructure and Mechanical Properties of PCTG-Based Nanocomposites

A. Granado, J. I. Eguiazábal, J. Nazábal

Departamento de Ciencia y Tecnología de Polímeros and Instituto de Materiales Poliméricos "POLYMAT," Facultad de Química, UPV/EHU, P. O. Box 1072, 20080 San Sebastián, Spain

Correspondence to: J. I. Eguiazábal (E-mail: josei.eguiazabal@ehu.es)

ABSTRACT: The influence of the processing temperature on both the dispersion level and the mechanical properties of the amorphous copolyester (PCTG)/organoclay (Cloisite® 20A) nanocomposite (NC) is studied in this article. At high processing temperatures, no change in the chemical nature of the matrix was observed, but its molecular weight decreased. Widely dispersed structures were observed by wide angle X-ray diffraction (WAXD) and transmission electron microscopy whatever the processing temperature might be. Dispersion was greatest for the samples processed at 200°C due to the highest viscosity of these samples and decreased at higher processing temperatures (T_p). These different dispersion levels led to a large modulus increase (71%) after processing at 200°C and to lower ones (about 50%) after processing at 230 and 260°C. The ductility of the NCs decreased at lower processing temperatures. The decrease was attributed to the greater stiffness of the matrix, and was not significant enough to modify the ductile nature of the NCs, which showed clear yield points even at the lowest processing temperature (200°C). © 2012 Wiley Periodicals, Inc. J. Appl. Polym. Sci. 000: 000–000, 2012

KEYWORDS: mechanical properties; nanocomposites; polyesters

Received 15 December 2010; accepted 28 March 2012; published online
DOI: 10.1002/app.37810

INTRODUCTION

Polymer nanocomposites (NCs) based on layered silicates have generated a great deal of interest in recent years in both industrial and academic research.[1] This is because the high rigidity and aspect ratio of the clay particles, when well dispersed, lead to remarkable improvements in several properties, in particular mechanical and barrier as well as fire performance. Moreover, these improved properties are obtained at low filler loadings compared with those of conventional microcomposites. The melt intercalation method nowadays appears to be the most effective way to produce NCs,[2] as the mixing-induced shear stresses aid dispersion.[3] This is true provided favorable interaction occurs between the polymer and the organoclay.[2]

In the case of polymers that require high melt processing temperatures, thermal stability of the organic modifier (surfactant) of the montmorillonite clay, often an alkyl ammonium compound, is critical, which is why it is an important subject for research.[4–8] Thermogravimetric analysis (TGA) shows that the surfactant begins to break down at temperatures as low as 180°C under nonoxidative environments and that significant degradation may also occur just above this temperature.[4] Chemical degradation of the surfactant may affect[5] the dynamics of polymer intercalation and exfoliation as well as the interfacial bonding; obviously, these parameters clearly influence the physical and mechanical properties. In addition, surfactant degradation may cause unwanted secondary reactions with the matrix itself. Consequently, there exists a need to understand how the surfactant degrades and to analyze the conditions that cause it and how these conditions affect dispersion and the properties of the organoclay.

The effects of organoclay degradation have been studied in NCs based on polycarbonate (PC),[9] polyethylene (PE),[10,11] polypropylene,[11,12] polystyrene, high-impact polystyrene, poly(methyl methacrylate), acrylonitrile-butadiene-styrene terpolymer,[11] polyamide 12 (PA12),[13,14] poly(ethylene glycol),[15] poly(ε-caprolactone),[16] and on PA6/PE,[17] PA12/PE,[18] and PC/poly(butylene terephthalate) (PBT) blends,[19] but studies are more common in the case of poly(ethylene terephthalate) (PET)[20–22] and polyamide 6 (PA6)-based NCs.[4,23,24] Both in PET and PA6 NCs, significant matrix degradation occurs during melt mixing, which leads to both a decrease in molecular weight[4,20,21,23] and color formation.[4,21–23] The influence of clay dispersion on degradation,[21]

the chemical structure of the surfactant,[4,21] the characteristics of the polymer,[4] and the water content[24] have all been studied. Both a thermally stable surfactant[25] for PET-based NCs and an antioxidant for PA6 NCs[4] have been used.

The NCs of traditional packaging polymers like PET are very interesting from an applied point of view, mainly taking into account the improvements that clay particles lead to in barriers properties. However, due to the high processing temperatures of PET and the low degradation temperatures of the NCs, polymers with a lower processing temperature should be of clear interest. In this way, an amorphous copolyester derived from PET, poly(ethylene glycol-co-cyclohexane-1,4-dimethanol terephthalate) (PCTG), has a lower processing temperature and it is also very useful especially because of its clarity, transparency, and toughness in applications such as blister packaging and bags.* For this reason, it could lead to interesting NCs. These NCs have been recently prepared and characterized in our laboratory[26] and showed favorable mechanical behavior. However, the effects of possible degradation during the processing of these NCs had not, to our knowledge, been studied. Thus, the aim of this article is to examine the effects of the T_p (200, 230, and 260°C) on the structure and mechanical properties of PCTG-based NCs. As it is known, a change in the processing temperature leads to two possible effects on the structure. There are a change in the orientation and a possible degradation. Neat PCTG was also processed under the same conditions as a reference material.

EXPERIMENTAL

The polymer used in this work is an amorphous copolyester (T_g = 84.5°C), Eastar PCTG DN011 (PCTG), from Eastman (Middelburg, Netherlands). Its chemical structure is represented in Figure 1. The filler (Cloisite® 20A, Southern Clay Products (Gonzalez, Texas)) is a montmorillonite modified with dimethyl dehydrogenated-tallow quaternary ammonium (OMMT). The percentage of weight loss on ignition is 38% and the dry particle sizes, in volume, is 10% less than 2 μm, 50% less than 6 μm, and 90% less than 14 μm.† Drying before processing was performed in an air-circulation oven at 65°C for 6 h for PCTG and at 80°C for 4 h in the case of the OMMT.

The NCs with a weight and a volume content of 5 and 2.8% Cloisite® 20A, respectively, were processed in a Collin (Ebersberg, Germany) ZK25 corotating twin-screw extruder-kneader. The diameter of the screws and the L/D ratio was 25 mm and 30, respectively. The rotation speed was 200 rpm, the flow rate 1.13 cm^3/s, and the barrel temperature 200°C, to prevent any significant degradation of the clay particles. The extrudates were cooled in a water bath, pelletized, and dried for 24 h at 65°C. Injection molding of the NCs and of the reference PCTG was carried out in a Battenfeld (Meinerzhagen, Germany) BA-230E reciprocating screw injection molding machine to obtain tensile (ASTM D638, Type IV, thickness 2.05 mm) specimens. The screw of the plasticization unit was a standard screw with a diameter of 18 mm, L/D ratio of 17.8, and a compression ratio of 4. The melt temperatures were 200, 230, and 260°C and the mold temperature was 15°C. The injection pressure was 260 MPa and the correspondent injection speed was 11.4 cm^3/s.

*Technical information from Eastman.
†Technical information from Southern Clay Products.

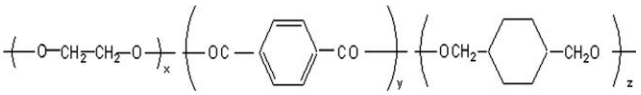

Figure 1. Chemical structure of the amorphous copolyester (PCTG).

Dynamic mechanical analysis was performed using a TA Q800 (Wilmington, DE) DMA that provided the loss tangent (tan δ) (accuracy ±0.01) and the storage modulus (E') (accuracy ±5%) against temperature. The scans were carried out in bending mode at a constant heating rate of 4°C/min and at a frequency of 1 Hz, from 30°C to roughly 120°C. The glass transition temperature (T_g) was measured as the temperature at which the maximum of the tan δ plots appeared. The T_g was also studied by differential scanning calorimetry (DSC). The DSC scans were carried out using a Perkin-Elmer DSC-7 (Norwalk, CT) calorimeter at a heating rate of 20°C/min in a nitrogen atmosphere. Two heating scans were carried out between 25 and 125°C. Cooling between both scans was carried out at the maximum rate provided by the calorimeter. The T_g's were determined in the second scans.

Infrared analysis of the samples was performed in a Nicolet Magna (Ramsey, Minnesota) IR 560 spectrophotometer (accuracy ±0.35) with an attenuated total reflectance objective. The samples were obtained from the injection molded tensile specimens. TGA measurements were carried out using a TA Instruments (Wilmington, DE) thermobalance, TGA Q500 (accuracy $<$ ±0.1% in the balance mechanism), under air atmosphere and at a heating rate of 10°C/min, which are the conditions used in the reviewed articles.[22] The flow rate of gases into the cell for TGA was 75 mL/min and the nitrogen flow rate for purge was 50 mL/min. Birefringence was measured on thin sections of the specimens (thickness of roughly 0.7–0.8 mm) at room temperature in an Olympus (Champaign, IL) BX40 polarized light microscope (accuracy ±0.001) equipped with a compensator. Each birefringence value was obtained from a minimum of three measurements.

The molecular weight of the matrix was studied by solution viscosimetry as it is the most sensitive technique for measuring M_n in NCs, as gel permeation chromatography is virtually unworkable due to the presence of inorganic nanoparticles. The relative viscosity (η_{rel}), defined as the ratio of the solution flow time to solvent flow time, was measured using an Ubbelohde capillary viscometer at 35°C. The samples were dissolved in a mixture of phenol and 1,1,2,2-tetrachloroethane (40 : 60 by weight). The intrinsic viscosity was determined as the middle point between the $(\eta_{rel} - 1)/C$ and ln η_{rel}/C values, where C is the solution concentration. The viscosity average molecular weight, M_{η}, was determined from the Mark–Houwink relation, $[\eta] = KM_{\eta}^{\alpha}$, where K and α are specific constants for fixed conditions of polymer, solvent, and temperature. The K and α values for PCTG were not found, but taking into account that PCTG is a PET derivate polymer and that only an estimation of the qualitative behavior of the molecular weight as a function of the

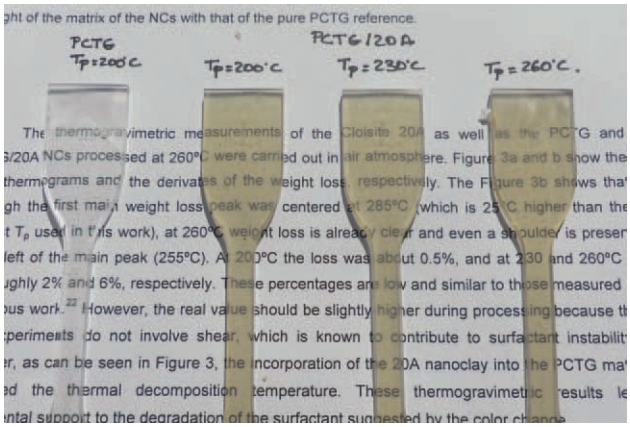

Figure 2. Tensile specimens of the PCTG molded at 200°C and those of the PCTG/20A NCs molded at 200, 230, and 260°C. [Color figure can be viewed in the online issue, which is available at wileyonlinelibrary.com.]

processing temperature is required, K and α values for PET in this solvent and temperature, $K = 1.25 \times 10^{-3}$ dL/g and $\alpha = 0.65$, were used.[27]

X-ray diffraction patterns were recorded on a Bruker (Karlsruhe, Germany) D8 diffractometer (accuracy ±0.0001°) operating at 45 kV and 50 mA, using a Ni-filtered CuKα radiation source (λ = 0.15406 nm). The transmission electron microscopy (TEM) samples were ultrathin sectioned at 150–200 nm using an ultramicrotome. The micrographs were obtained in a Philips Tecnai (Eindhoven, Netherlands) G2 20 twin microscope at an accelerating voltage of 200 kV. The average number of platelets per particle (n) was measured from TEM micrographs and was calculated as follows:

$$n = \frac{\sum n_t n_p}{\sum n_p} \quad (1)$$

where n_p is the number of particles with n_t number of platelets.

Tensile testing was carried out using an Instron (High Wycombe, UK) 5569 machine (accuracy ±0.25% of the measured load), at a cross-head speed of 10 mm/min, at 23 ± 2°C and 50 ± 5% relative humidity. The mechanical properties (yield and break stresses and ductility, measured as the break strain) were determined from the load–displacement curves. Young's modulus was determined by means of an extensometer at a crosshead speed of 1 mm/min. Ductility was also measured by means of the reduction of the transversal area on fracture using the expression:

$$D = \frac{A_0 - A}{A_0} \times 100 \quad (2)$$

where D is ductility and A_0 and A are the initial and final transversal areas of the specimens, respectively. A minimum of eight tensile specimens were tested for each reported value.

RESULTS AND DISCUSSION

It is known[4,8] that in the case of NCs, in addition to the possible degradation of the matrix itself, the surfactant of the organoclay may also degrade during processing. After processing and irrespective of the processing temperature (T_p), it can be seen that the transparent NCs specimens darkened showing a yellowish/brownish color (Figure 2). Similar changes were observed in PET/Cloisite® 20A NCs.[22] As no change of color was seen in the neat polymer, the color change indicates that some organoclay-induced degradation occurred. For this reason, the possible degradation of the surfactant of the Cloisite® 20A was studied by thermogravimetric measurements and the possible extent of the degradation of the matrix was studied by comparing the molecular weight of the matrix of the NCs with that of the pure PCTG reference.

The thermogravimetric measurements of the Cloisite® 20A as well as the PCTG and PCTG/20A NCs processed at 260°C were carried out in air atmosphere. Figure 3(a, b) shows the TGA thermograms and the derivates of the weight loss, respectively. Figure 3(b) shows that although the first main weight loss peak was centered at 285°C (which is 25°C higher than the highest T_p used in this work), at 260°C, weight loss is already clear and even a shoulder is present at the left of the main peak (255°C).

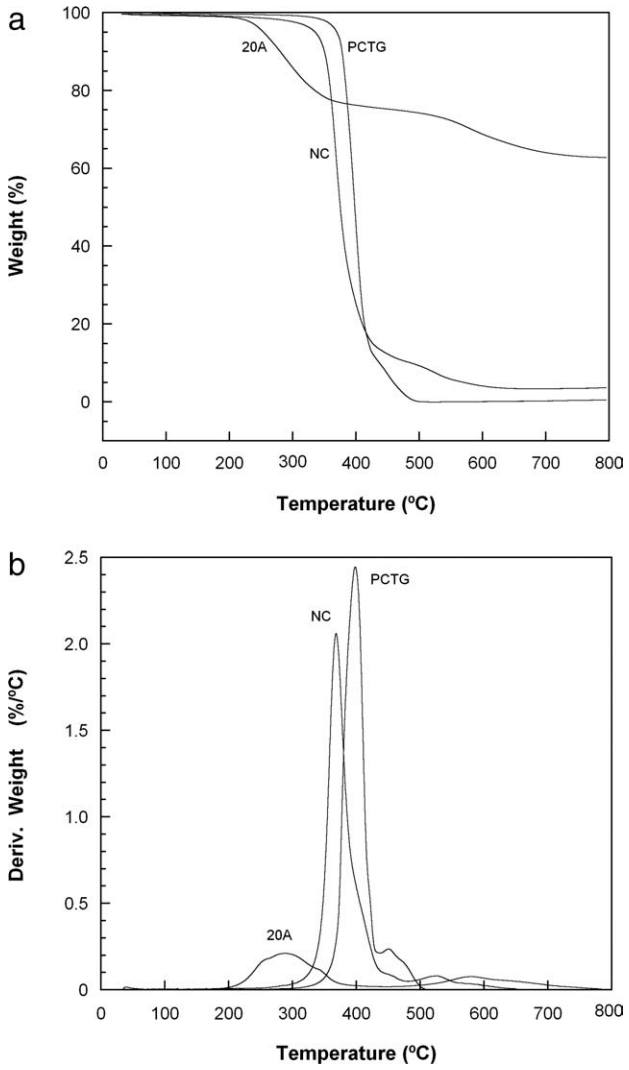

Figure 3. TGA curves (a) and loss weight derivates (b) of the Cloisite® 20A, PCTG, and PCTG/20A NC processed at 260°C, under air.

Applied Polymer SCIENCE

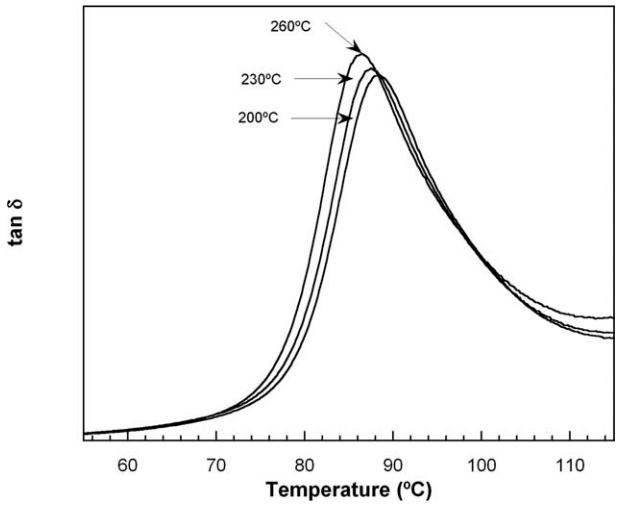

Figure 4. Temperature dependence of tan δ for PCTG/20A NCs at different T_p's.

At 200°C, the loss was about 0.5%, and at 230 and 260°C, it was roughly 2 and 6%, respectively. These percentages are low and similar to those measured in a previous work.[22] However, the real value should be slightly higher during processing because the TGA experiments do not involve shear, which is known to contribute to surfactant instability.[4] Moreover, as can be seen in Figure 3, the incorporation of the 20A nanoclay into the PCTG matrix decreased the thermal decomposition temperature. These thermogravimetric results lend experimental support to the degradation of the surfactant suggested by the color change.

Before studying the molecular weight (M_n) of the polymer matrix of the NCs by solution viscosimetry, it is important to bear in mind that viscosity may change due to other effects. Thus, a possible change in viscosity could be due to a decrease in M_n.

Table I. Intrinsic Viscosity (η) (dL/g) and Viscosity Average Molecular Weight (M_η) (g/mol) of PCTG and PCTG/20A NCs after Injection Molding at Different Processing Temperatures and Those of the NCs after Extrusion (NC_{ext})

Sample	200°C	230°C	260°C
NC_{ext} (η)	0.80	-	-
NC (η)	0.91	0.83	0.85
PCTG (η)	0.97	0.89	0.87
NC_{ext} (M_η)	20,900	-	-
NC (M_η)	25,300	22,000	22,800
PCTG (M_η)	27,900	24,500	23,600

Moreover, possible surfactant migration, which should lead to plasticization, could also lead to a decrease in viscosity. To evaluate the possible surfactant migration, the glass transition temperature (T_g) of the NCs was evaluated. The T_g of the NCs, measured from the maximum of the tan δ plots (Figure 4), showed a slight tendency to decrease when the T_p increased. The T_g was also measured by DSC showing the same tendency as tan δ, that is, a slight decrease (from 84.6 to 83.4°C) was appreciated as the processing temperature increased (from 200 to 260°C). The changes were very small (less than 2°C) and scarcely significant as they are close to the error of measurement. However, the intensity of the tan δ peaks of the NCs increased, and the peaks widened after processing at high temperatures. This indicates[28] interaction between the polymer matrix and the clay layers resulting in the reduction of internal friction and the immobilization of the polymer chains. Thus, while some surfactant migration occurred, it must have been too small to influence viscosity because the T_g hardly changed.

Although less likely, a possible change in the chemical nature of the NCs could alter viscosity, and so should also be tested. For

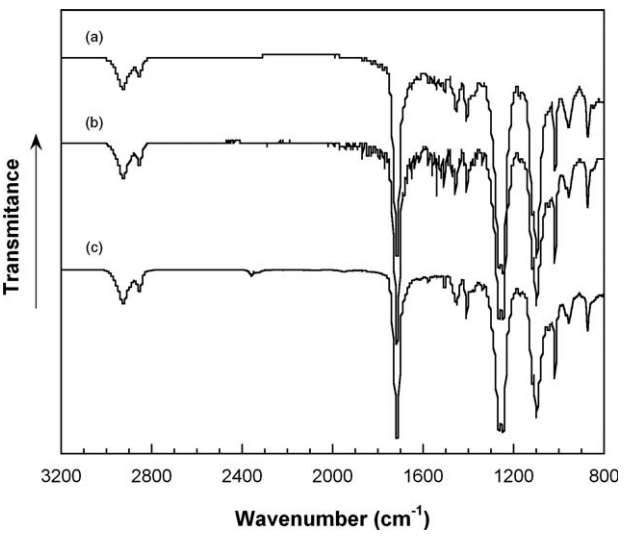

Figure 5. FTIR spectra of the PCTG pellets (a) and PCTG/20A NCs processed at 200°C (b) and 260°C (c).

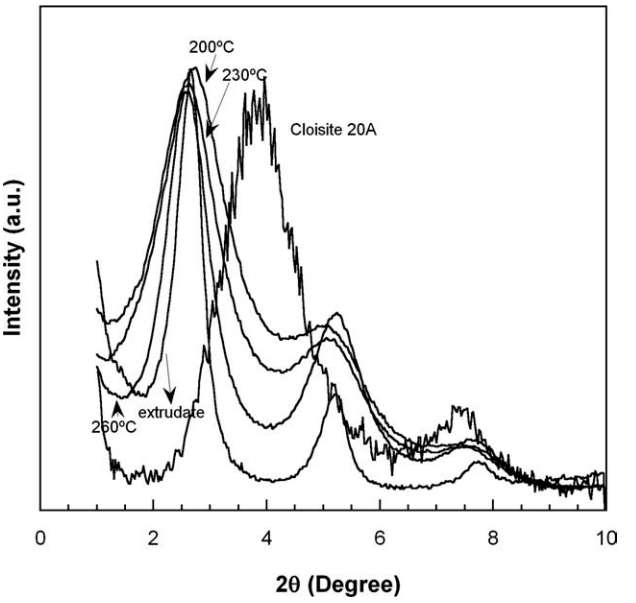

Figure 6. WAXD patterns of the Cloisite® 20A, PCTG/20A extrudate, and PCTG/20A NCs at different T_p's.

Table II. Position of the Main Peaks of the Specimens on the WAXD Scans and the Corresponding Basal Distance

Specimen	Position of the main peak (°)	d_{001} (nm)
Cloisite 20A	3.86	2.29
PCTG/20A ($T_p = 200$°C)	2.72	3.25
PCTG/20A ($T_p = 230$°C)	2.60	3.40
PCTG/20A ($T_p = 260$°C)	2.60	3.40

this reason, the FTIR spectrum of the NC processed at 260°C (where a possible reaction is most probable) is compared in Figure 5 with that of the NC processed at 200°C and also with that of the PCTG pellets. As can be seen, no remarkable change was observable between the spectra of the NCs processed at 200 and 260°C and even the spectrum of the pellets remained the same. Consequently, the M_n of the NCs can be calculated from the viscosity values.

The intrinsic viscosity (η) and viscosity average molecular weight (M_η) of both the NCs and the reference PCTG after processing at different temperatures are listed in Table I. As can be seen, the viscosity of the molded samples increased with respect to that of the extrudate. As it is known,[29,30] during processing of some aromatic polymers, both chain extension or chain scission can occur. The initial molecular weight increase seemed to indicate that in PCTG at low processing temperatures, esterification or transesterification prevailed against chain scission. Moreover, Table I illustrates how the viscosity and consequently the calculated M_η decreased from over 25,000 to just over 22,000 (a 0.02 change in viscosity is close to the accuracy of the measurement) when T_p increased from 200°C to either 230 or 260°C. The change of η with T_p was similar to that of the reference PCTG: η decreased when T_p changed from 200 to 230°C, but remained roughly the same when T_p increased to 260°C. In addition, the values of the NCs were smaller than those of the pure PCTG. As the only difference is the presence of the clay, this indicated that clay particles were involved in the degradation of the matrix.

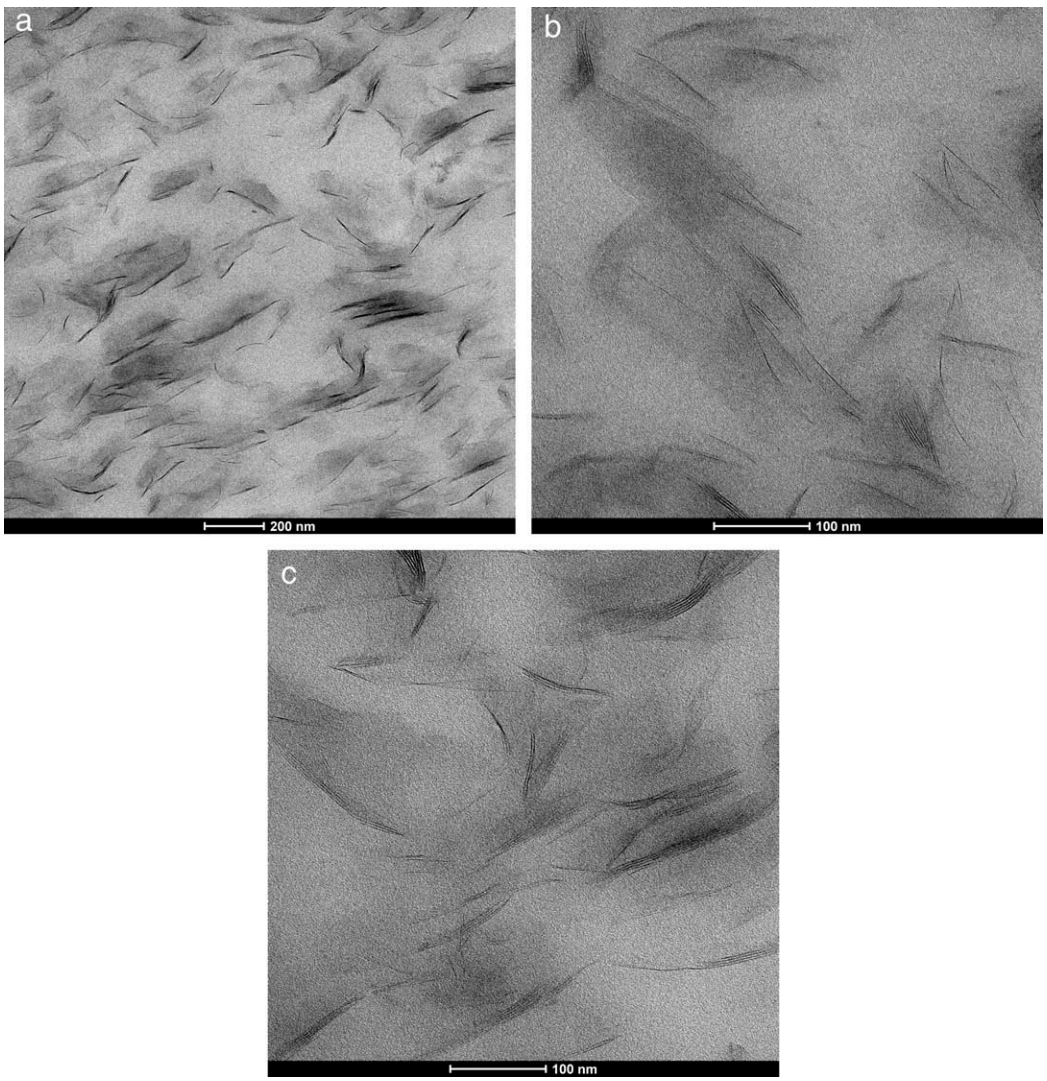

Figure 7. TEM photomicrographs of (a) the PCTG NC processed at 260°C at low magnification, and processed at 200°C (b) and 260°C (c) at high magnification.

The decrease in η at increasing T_p indicates that chain scission occurred and that it was greater as T_p increased.

Nanostructure

The nanostructure of the NCs was studied by both WAXD and TEM. In Figure 6, the WAXD scans of the Cloisite® 20A and of the NCs are shown and the results of the position of the main peak of the specimens and the corresponding basal distance are shown in Table II. As can be seen, the scan of the Cloisite® 20A shows the peak characteristic of the (001) plane at 3.86°, which, according to Bragg's law, corresponds to a basal distance, d_{001} of 2.29 nm. The position of the main peak of the NCs clearly shifted to smaller 2θ values indicating intercalation. This intercalation level ($\Delta d_{001} = 0.96$ for samples processed at 200°C and 1.11 for samples processed at 230 and 260°C) is comparable with those of PET-based (0.92)[31] and poly(trimethylene terephthalate) (PTT)-based (0.57 with 20A and 1.17 with 30B) NCs.[32] Moreover, the main peak of the NC processed at 200°C appeared at 2.72° ($d_{001} = 3.25$ nm), whereas the peaks of the NCs obtained at 230 and 260°C were centered at 2.60° ($d_{001} =$ 3.40 nm). This indicates a larger Δd_{001} and intercalation at high T_p's, which may be due to different causes. A degradation-induced decrease in molecular weight[33] could be the cause of the higher intercalation but the opposite has also been claimed.[34] Another possibility is that the clay galleries expanded due to volatiles generated during possible surfactant degradation.[5] In these NCs, taking into account the slight surfactant degradation deduced from thermogravimetric measurements, it seems to be the reason for the expansion of the galleries.

The nanostructure of the NCs was also studied by TEM, and the results are shown in Figure 7. The morphology of the NC processed at 260°C at low magnification [Figure 7(a)] showed good dispersion with a mixed intercalated/exfoliated nanostructure where intercalated nanostructures prevailed. At low magnification, no clear differences were observed when T_p changed. However, at high magnification [Figure 7(b, c), $T_p =$ 200 and 260°C, respectively], a slightly higher dispersion level at 200°C [Figure 7(b)] seemed to exist because the number of platelets per particle at 260°C appeared to be higher. To test this preliminary impression, the degree of dispersion of the NCs was measured by calculating the number of platelets per particle (n) from TEM micrographs. For each measurement, more than 10 pictures were analyzed. The results are shown in Figure 8(a–c). As can be seen, the average number of platelets per particle increased with T_p from 2.4 at $T_p = 200$°C to 2.7 and 3.4 at T_p of 230 and 260°C, respectively. Moreover, the amount of individual layers (28, 25, and 15% in the NCs processed at 200, 230, and 260°C, respectively) also decreased when T_p increased. Both data prove that at higher T_p's, the dispersion level is poorer. This is attributed[35–37] to the lower melt viscosity of the molten matrix at higher T_p's, which leads to lower shear stress during blending which, in turn, hinders exfoliation.

Mechanical Properties

Figure 9 shows the modulus of elasticity and the yield stress of the NCs as well as those of the neat PCTG as a function of T_p. It can be observed that the modulus of elasticity clearly

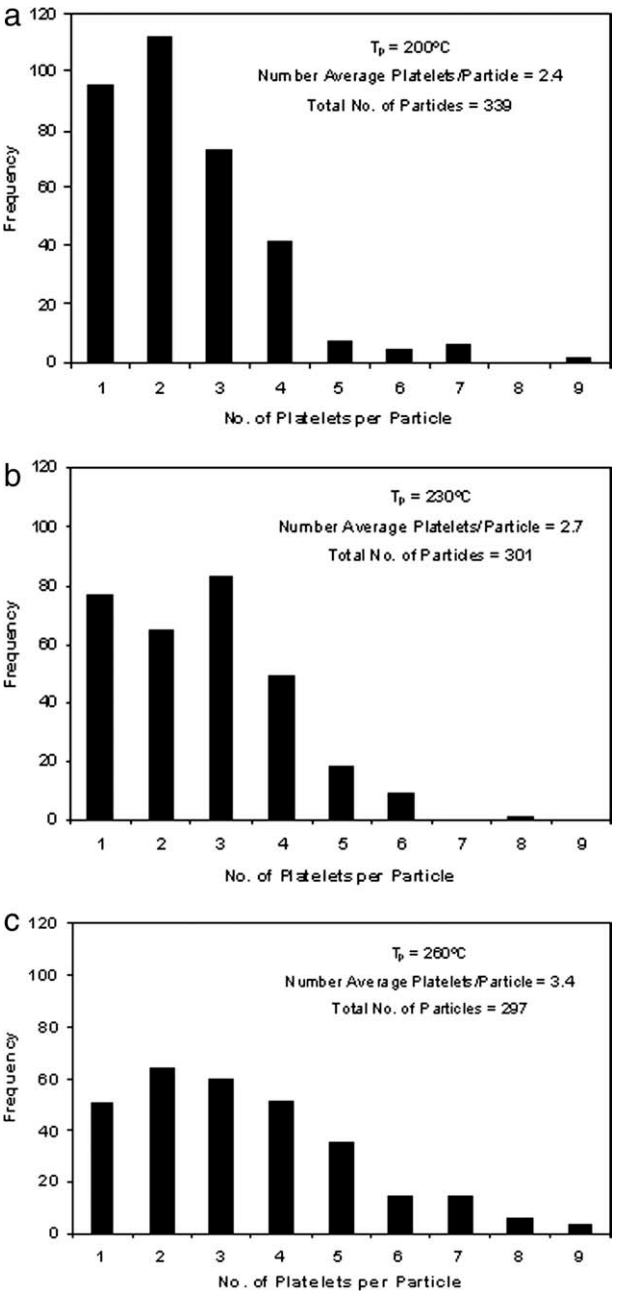

Figure 8. Histograms of the NCs number of platelets per particle, for samples processed at (a) 200°C (b) 230°C, and (c) 260°C.

increased after the addition of the nanoclay. The storage modulus (E') (Figure 10) also increased when the organoclay was added. The modulus increases (Figure 9) in the NCs were large: 72% after processing at 200°C and 52% after processing at 230 and 260°C. This is attributed, both in the case of the modulus of elasticity and of the storage modulus, to physical interaction between the organoclay and the matrix that led to the stiffening of the matrix.[38,39] The modulus of elasticity increases are comparable to those obtained in the most successful PA6-based NCs with Cloisite® 20A or trimethyl hydrogenated-tallow ammonium montmorillonite.[36] These modulus increases and those

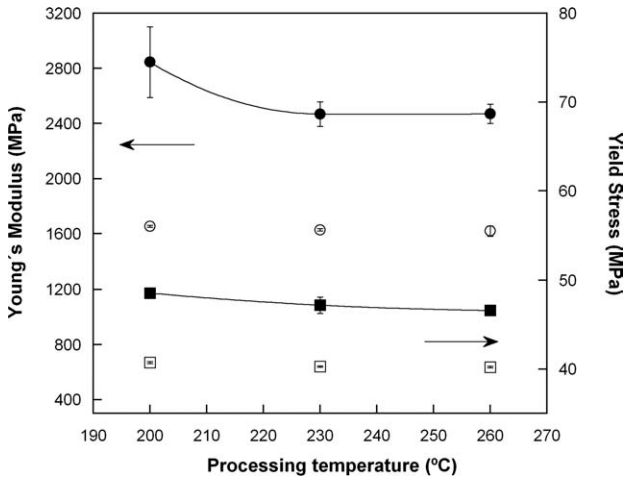

Figure 9. Young's modulus (○) and yield stress (□) of neat PCTG (white symbols) and PCTG/20A (black symbols) as a function of the T_p's.

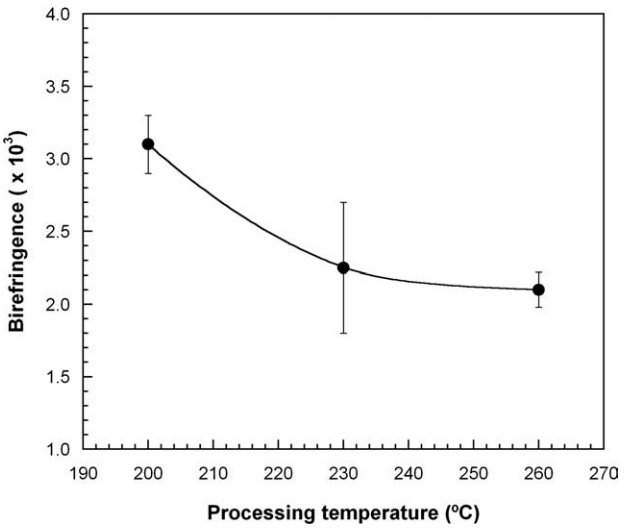

Figure 11. Birefringence of PCTG/20A NCs as a function of the T_p's.

obtained in other NCs based on polyesters are compared. The increases contained in this work are significantly greater than those observed in PET- and PTT-based NCs with 5% Cloisite® 20A (35 and 42%, respectively)[31,32] and comparable to those obtained previously for NCs based on PCTG.[26]

As Figure 10 shows, the E' values decreased when T_p changed from 200 to 230°C, but the decrease was almost imperceptible when T_p changed to 260°C. This is exactly the behavior observed in the plot of the modulus of elasticity in Figure 9 and increases the reliability of the observed dependence. In the case of E', the effect extended up to the T_g, as two parameters showed the same behavior, a decrease with T_p increasing. The changes in small strain properties of NCs, ruling out the presence of significant surfactant contents that would decrease the modulus, should be mainly associated with the dispersion/exfoliation level and with orientation. For this reason, to isolate the effect of the clay on the modulus using the orientation parameter, the global orientation was estimated by means of birefringence measurements in a polarized light microscope, and the results are shown in Figure 11. As can be seen, the birefringence of the NCs, and consequently the orientation, decreased at increasing T_p. Moreover, the orientation behavior was fairly similar to that of the modulus, because the birefringence decrease was high when the T_p changed from 200 to 230°C, but it almost remained stable when T_p changed to 260°C. These changes in orientation, however, while qualitatively similar to those of the modulus, are quantitatively too small to be solely responsible for the observed modulus changes.

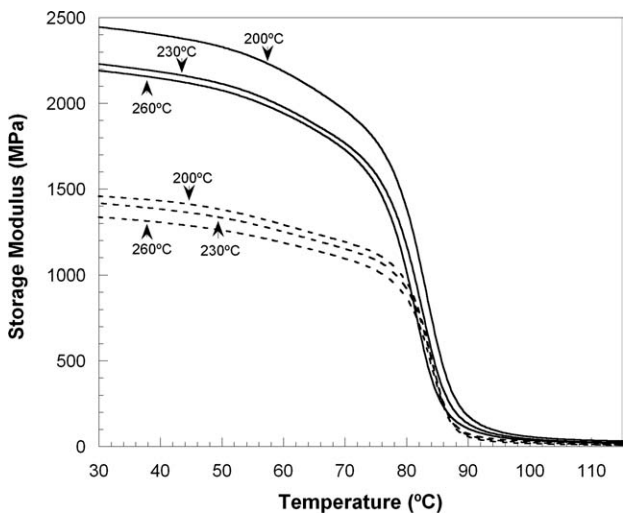

Figure 10. Temperature dependence of dynamic storage modulus (E') for PCTG/20A NCs (continuous line) and neat PCTG (dashed line) at different T_p's.

With respect to the dispersion level, the highest modulus value (NCs at $T_p = 200$°C) was in keeping with the highest dispersion and exfoliation levels [Figure 8(a)] of these NCs. This is because higher exfoliation/dispersion levels lead to a higher contact area, thus strengthening the polymer.[1,3] Therefore, the decrease in the dispersion level with the T_p increase (Figure 8) is proposed as being the main factor responsible for the modulus decrease. However, the relationship between the dispersion level and the modulus is not exact throughout since, while the relevant modulus change is seen when the T_p varied from 200 to 230°C, that of the dispersion level is observed between T_p values of 230 and 260°C. This may be due to orientation, which also influences its behavior.

Table III. Ductility of the Samples (%) Measured as the Elongation at Break (ε_b) and as the Reduction of the Transversal Area upon Fracture (ε_t) at Different Processing Temperatures

	Temperature (°C)		
	200	230	260
ε_b	44	66	135
ε_t	55	55	60

The yield stress (Figure 9) of the PCTG also remained constant with T_p, and its behavior after the addition of the nanoclay was, as to be expected, qualitatively similar to that of the modulus. In keeping with previous results,[26] the increases were clearly smaller than those of the modulus.

As can be seen in Table III, the ductility values, measured as the elongation at break, changed from 44% at $T_p = 200°C$ to 66 and 135% at $T_p = 230$ and 260°C, respectively. The lowest ductility value after a $T_p = 200°C$ is consistent[36] with the greater stiffness observed at lower T_p's. The real ductility changes, however, are small. This is because the change in ductility measured as the reduction of the transversal area upon fracture [eq. (2)] was very low (Table III). This small change is attributed to the fact that, in NCs, the presence of large particles has hardly any effect on ductility; this is because even the largest nanoscopic particles are not big enough to create stress concentrations that would lead to more accelerated fracturing.

CONCLUSIONS

The lowest T_p (200°C) led to the best dispersion in the PCTG NCs, as the amount of individual layers (28, 25, and 15% in the NCs processed at 200, 230, and 260°C, respectively) was the highest at this T_p. This is attributed to the greater viscosity induced shear stress.

The change of T_p gave rise to a degradation that was minimum at low T_p and was confirmed by a slight molecular weight decrease and a darkening of the specimens. The increase in the interlaminar gallery distance with T_p (from 3.25 nm at 200°C to 3.40 nm at 230 and 260°C) was also related with the degradation. This is because it is attributed to the generated volatiles, as established by thermogravimetry at the used T_p's. Degradation starts at low temperatures and appears to be mainly confined to the clay galleries as no negative effect on ductility was detected.

The greater dispersion had no significant effect on the T_g, but led to rather relevant modulus increases of 72% at 200°C and 52% at 230 and 260°C. The increase in the modulus is mainly related to the better dispersion of the NCs processed at lower temperatures and to a lesser extent to the slight change of the orientation.

Based on the results of this work, the lower T_p, that is, 200°C, despite the lower ductility that it leads to, is considered the best processing temperature for these NCs. This is due to the large dispersion and lower degradation of the NCs processed at this temperature. Moreover, these NCs compared with PET NCs showed similar dispersion level and higher modulus.

ACKNOWLEDGMENTS

The financial support of the Basque Government (Project No. S-PE11UN050) is gratefully acknowledged.

REFERENCES

1. Utracki, L. A. Clay-Containing Polymeric Nanocomposites; Rapra Technology: Shropshire, **2004.**
2. Cho, J. W.; Paul, D. R. *Polymer* **2001,** *42*, 1083.
3. Dennis, H. R.; Hunter, D. L.; Chang, D.; Kim, S.; White, J. L.; Cho, J. W.; Paul, D. R. *Polymer* **2001,** *42*, 9513.
4. Fornes, T. D.; Yoon, P. J.; Paul, D. R. *Polymer* **2003,** *44*, 7545.
5. Xie, W.; Gao, Z.; Pan, W. P.; Hunter, D.; Singh, A.; Vaia, R. *Chem. Mater.* **2001,** *13*, 2979.
6. Cervantes-Uc, J. M.; Cauich-Rodríguez, J. V.; Vázquez-Torres, H.; Garfias-Mesias, L. F.; Paul, D. R. *Thermochim. Acta* **2007,** *457*, 92.
7. Gelfer, M.; Burger, C.; Fadeev, A.; Sics, I.; Chu, B.; Hsiao, B. S.; Heintz, A.; Kojo, K.; Hsu, S.-L.; Si, M.; Rafailovich, M. *Langmuir* **2004,** *20*, 3746.
8. Cui, L.; Khramo, D. M.; Bielawski, C. W.; Hunter, D. L.; Yoon, P. J.; Paul, D. R. *Polymer* **2008,** *49*, 3751.
9. Yoon, P. J.; Hunter, D. L.; Paul, D. R. *Polymer* **2003,** *44*, 5341.
10. Dintcheva, N. T.; Al-Malaika, S.; La Mantia, F. P. *Polym. Degrad. Stab.* **2009,** *94*, 1571.
11. Su, S.; Wilkie, C. A. *Polym. Degrad. Stab.* **2004,** *83*, 347.
12. Tang, Y.; Hu, Y.; Song, L.; Zong, R.; Gui, Z.; Chen, Z.; Fan, W. *Polym. Degrad. Stab.* **2003,** *82*, 127.
13. Méderic, P.; Razafinimaro, T.; Aubry, T. *Polym. Eng. Sci.* **2006,** *46*, 986.
14. Méderic, P.; Razafinimaro, T.; Aubry, T., Moan, M., Klopffer, M.-H. *Macromol. Symp.* **2005,** *221*, 75.
15. Chen, B.; Evans, J. R. G.; Holding, S. *J. Appl. Polym. Sci.* **2004,** *94*, 548.
16. Chrissafis, K.; Antoniadis, G.; Paraskevopoulos, K. M.; Vassiliou, A.; Bikiaris, D. N. *Comp. Sci. Tech.* **2007,** *67*, 2165.
17. Scalfaro, R.; Mistretta, M. C.; La Mantia, F. P. *Polym. Degrad. Stab.* **2008,** *93*, 1267.
18. Méderic, P.; Ville, J.; Huitric, J.; Moan, M.; Aubry, T. *Polym. Eng. Sci.* **2011,** *51*, 969.
19. Polo, W. S. D.; Litchfield, D. W.; Baird, D. G. *Annu Tech Conf-Soc Plast Eng* **2006,** *64*, 2330.
20. Patro, T. U.; Khakhar, D. V.; Misra, A. *J. Appl. Polym. Sci.* **2009,** *113*, 1720.
21. Xu, X.; Ding, Y.; Qian, Z.; Wang, F.; Wen, B.; Zhou, H.; Zhang, S.; Yang, M. *Polym. Degrad. Stab.* **2009,** *94*, 113.
22. Stoeffler, K.; Lafleur, P. G.; Denault, J. *Polym. Degrad. Stab.* **2008,** *93*, 1332.
23. Ito, M.; Nagai, K. *J. Appl. Polym. Sci.* **2008,** *108*, 3487.
24. Davis, R. D.; Gilman, J. W.; VanderHart, D. L. *Polym. Degrad. Stab.* **2002,** *79*, 111.
25. Costache, M. C.; Heidecker, M. J.; Manias, E.; Wilkie, C. A. *Polym. Adv. Technol.* **2006,** *17*, 764.
26. González, I.; Eguiazábal, J. I.; Nazábal, J. *Macromol. Mater. Eng.* **2008,** *293*, 781.
27. Brandrup, J.; Immergut, E. H.; Grulke, E. A. Polymer Handbook; Willey: New Jersey, **1999.**
28. Kalgaonkar, R. A.; Jog, J. P. *J. Polym. Sci.: Polym. Phys.* **2008,** *46*, 2539.
29. Paci, M.; La Mantia, F. P. *Polym. Degrad. Stab.* **1998,** *61*, 417.

30. Kuroda, S.-I.; Terauchi, K.; Nogami, K.; Mita, I. *Eur. Polym. J.* **1989,** *25*, 1.
31. Gurmendi, U.; Eguiazábal, J. I.; Nazábal, J. *Macromol. Mater. Eng.* **2007,** *292*, 169.
32. Gurmendi, U.; Eguiazábal, J. I.; Nazábal, J. *Eur. Polym. J.* **2008,** *44*, 1686.
33. Liaw, J. H.; Hsueh, T. Y.; Tang, T.-S.; Wang, Y.; Chiao, S.-M. *Polym. Int.* **2007,** *56*, 1045.
34. Chau, D.; Nguyen, Q.; Baird, D. G. *Polym. Compos.* **2007,** *28*, 499.
35. Yoon, P. J.; Hunter, D. L.; Paul, D. R. *Polymer* **2003,** *44*, 5323.
36. Fornes, T. D.; Yoon, P. J.; Hunter, D. L.; Keskkula, H.; Paul, D. R. *Polymer* **2002,** *43*, 5915.
37. Fornes, T. D.; Yoon, P. J.; Keskkula, H.; Paul, D. R. *Polymer* **2001,** *42*, 9929.
38. Kim, J. Y.; Kim, D. K.; Kim, S. H. *Polym. Compos.* **2009,** *30*, 1779.
39. Yao, X.; Tian, X.; Zhang, X.; Zheng, K.; Zheng, J.; Wang, R.; Kang, S.; Cui, P. *Polym. Eng. Sci.* **2009,** *49*, 799.